

# Aggregation-Induced Emission for Highly Selective and Sensitive Fluorescent Biosensing and Cell Imaging

Liang Huang, Liming Dai

Department of Macromolecular Science and Engineering, Center of Advanced Science and Engineering for Carbon (Case4carbon), Case Western Reserve University, 10900 Euclid Avenue, Cleveland, Ohio 44106  
Correspondence to: L. Dai (E-mail: liming.dai@case.edu)

Received 14 October 2016; accepted 14 November 2016; published online in Wiley Online Library

DOI: 10.1002/pola.28447

**ABSTRACT:** Fluorescent bioprobes are powerful analytical tools for studying biological activities in living systems. Fluorogens with aggregation-induced emission (AIE) characteristics have recently emerged as a new class of fluorescent bioprobes for biosensing and cell imaging. As discovered by Tang, AIE fluorogens are nearly nonemissive in molecular states with their intermolecular rotations being not restricted whereas their fluorescence is turned on by binding with certain biomolecules, leading to highly selective turn-on fluorescent probes for specific biomolecules and fluorescent cell imaging with a high signal-to-background noise ratio. By introducing the AIE characteristics into polymeric materials, AIE polymers could

possess a good solubility and biocompatibility, excellent structural diversity, and ease for functionalization useful for efficient biosensing and cell imaging. Herein, we highlight a few recently published articles on small and macromolecular AIE molecules to provide a fundamental understanding of the AIE mechanism and illustrate the working principle for AIE based biosensing and cell imaging. © 2017 Wiley Periodicals, Inc. *J. Polym. Sci., Part A: Polym. Chem.* **2017**, *55*, 653–659

**KEYWORDS:** aggregation-induced emission; biocompatibility; biological applications of polymers; biosensor; cell imaging; fluorescence; imaging; selectivity; sensitivity

**INTRODUCTION** Fluorescence emissions from conventional fluorophores are usually weakened or even quenched by aggregation at high concentrations,<sup>1</sup> known as concentration quenching or aggregation caused quenching (ACQ). For instance, *N,N*-dicyclohexyl-1,7-dibromo-3,4,9,10-perylene-tetracarboxylic diimide (DDPD), a well-known fluorophore, in tetrahydrofuran (THF, a good solvent for DDPD) at a low concentration (10  $\mu$ M) emits bright fluorescence under UV irradiation. In contrast, its fluorescence emission is weakened by adding water (a poor solvent for DDPD) into the solution and completely quenched when the water content reaches up to 70 vol % due to aggregation [Fig. 1(a)].<sup>2,3</sup> In the aggregate state, DDPD molecules stack together via strong  $\pi$ - $\pi$  interactions of the constituent perylene rings [Fig. 1(b)] to facilitate the nonradiative decay of the excited states, and hence the fluorescence emission quenching. Such an ACQ effect is ubiquitous, particularly for conventional luminophores comprised of planar aromatic rings.<sup>3,5</sup>

Fluorescent bioprobes are useful for directly detecting biomolecules *in vivo* and real-time visualizing complex cellular structures and processes.<sup>2,5</sup> For practical applications, high selectivity and sensitivity are necessary for fluorescent bioprobes.<sup>2</sup> The selectivity is determined mainly by affinity between the fluorescent bioprobe molecule and analyte

while the sensitivity depends strongly on the fluorescence brightness of the probe before and after its binding to an analyte.<sup>2</sup> Because of the ACQ effect, conventional fluorescent probes have to be used as isolated molecules at a low concentration in a fluorescence turn-off mode.<sup>2,3,5</sup> However, fluorescence emissions from dilute solutions are usually weak, leading to a poor sensitivity, and the use of a small amount of the probe molecules can easily cause photobleaching by a strong laser excitation. Furthermore, ACQ effect is even applicable to dilute solutions as small fluorescent molecules could accumulate to greatly increase the local concentration of the fluorescent probes to aggregate.<sup>2,3,5</sup> To mitigate luminogen aggregation, various chemical and physical approaches have been developed with limited success.<sup>5</sup>

In 2001, Ben Zhong Tang's group found that some silole derivatives exhibited weak or no fluorescence in a molecularly dissolved state, but emitted intense fluorescence once aggregated [Fig. 1(c)], leading to the discovery of the "aggregation-induced emission" (AIE).<sup>6</sup> The AIE effect was attributed to the restriction of intramolecular rotation (RIR).<sup>6</sup> As schematically shown in Figure 1(d) for hexaphenylsilole (HPS), fluorescent molecules with AIE characteristics usually have a propeller-shaped structure with rotating units (e.g. phenyl rings).<sup>3</sup> In a dilute solution, the fast motion

**Liang Huang** obtained his BS from Beijing University of Chemical Technology in 2011, and his PhD from Tsinghua University in 2016. He is currently a postdoctoral research associate in Professor Liming Dai's group at Case Western Reserve University. His current research interests are the fabrication of graphene-based membranes and their applications.



**Liming Dai** is Kent Hale Smith Professor at Case Western Reserve University and is also director of the Center of Advanced Science and Engineering for Carbon (Case4Carbon). He received a BSc from Zhejiang University in 1983, a PhD from Australian National University in 1991, and did his postdoctoral research at the Cavendish Laboratory in Cambridge. His research activities cover the synthesis and device fabrication of conjugated polymers and carbon nanomaterials for energy and bio-related applications.



of the rotating units leads to nonradiative decay of excited states, and hence nonemissive as molecular species. In contrast, the intramolecular motion of the rotating units is restricted in an aggregate state due to steric hindrance [Fig. 1(d)], opening the radiative pathway to induce bright fluorescence emission. So far, a large variety of AIE chromophores, including tetraphenylethene (TPE), triphenylphosphonium (TPP), and HPS, with a wide emission wavelengths ranging from visible to near-IR, have been developed.<sup>3,5,7</sup> Through modulation of the molecular rigidity, Tang and his coworkers have even demonstrated inter-transformation between the AIE and ACQ states for certain dyes.<sup>8</sup> Based on the RIR mechanism, Tang et al. have exploited various AIE fluorogens as turn-on bioprobes for biosensing and bioimaging.<sup>2,3,5,7,9,10</sup> Fluorescence of an AIE fluorogen could be turned on upon specific interaction with biomolecule(s) in a solution or inside of a cell, leading to a fluorescence turn-on biosensor. Compared to their fluorescence turn-off counterparts, the AIE-based turn-on sensors are more sensitive with a faster response and less false signal as the formation of even a few emissive aggregates can be readily identified by the naked eye from the dark background.<sup>2,11</sup> Another important class of fluorescent sensors with turn-on characteristic are chemical-reactive probes, which are non-emissive themselves, but could react with the analytes to yield the corresponding luminogens with high emission.<sup>12</sup>

Along with the great success in developing small AIE molecules, considerable progress has also been achieved for the exploration of AIE polymers.<sup>13,14</sup> Compared to small molecules, macromolecules possess many advantages, including numerous possibilities for chemical functionalization and physicochemical tuning their molecular structure, topology, and morphology, which otherwise are very difficult, if not impossible, to be realized with small molecule systems. AIE polymers can be synthesized by attaching AIE fluorogens onto polymer backbones or incorporating them as constituents in the main chains.<sup>13-15</sup> By introducing the AIE

characteristics into polymeric materials, AIE polymers could possess a good solubility and biocompatibility, excellent structural diversity, and ease for functionalization useful for efficient biosensing and cell imaging.<sup>16-21</sup> While a comprehensive review on the construction of AIE polymeric systems has been recently published by Tang et al.,<sup>14</sup> their potential applications for biosensing and cell imaging will be highlighted in appropriate sections of this article.

## RESULTS AND DISCUSSION

### AIE-Based Fluorescent Biosensing

Water solubility is a prerequisite for fluorescent probes in biosensors whereas most primary AIE fluorophores are hydrophobic.<sup>3-6,22</sup> Thus, research on the AIE-based fluorescent biosensing has recently extended to the modification of AIE dyes with appropriate hydrophilic functional groups.<sup>2,4,22</sup> In particular, Tang et al. functionalized HPS with amino groups, followed by protonization in hydrochloric acid.<sup>22,23</sup> The resultant A2HPS-HCl [Fig. 2(a)] are water-soluble and nonemissive in a dilute solution. Upon binding to proteins, DNA or RNA molecules, however, A2HPS-HCl becomes highly emissive because of the binding-induced restriction of its phenyl rotors. Therefore, A2HPS-HCl can be a promising turn-on fluorescent probe for biosensing. Like many other AIE fluorogens, the interactions of A2HPS-HCl with biomolecules often arise from the nonspecific electrostatic and/or hydrophobic forces, and hence poor or no selectivity to many bioanalytes. This has severely hindered practical application of AIE fluorogens for biosensing. In this context, Tang and co-workers used graphene oxide (GO) as a substrate to significantly enhance the selectivity of AIE fluorescent probes for certain biomolecules.<sup>23</sup> As illustrated in Figure 2(a), the positively charged A2HPS-HCl could adsorb onto GO through electrostatic and  $\pi$ - $\pi$  stacking interactions to form a stable non-emissive complex. Since the interaction of A2HPS-HCl with dsDNA is stronger than that with GO, the addition of the dsDNA could cause the release of the adsorbed

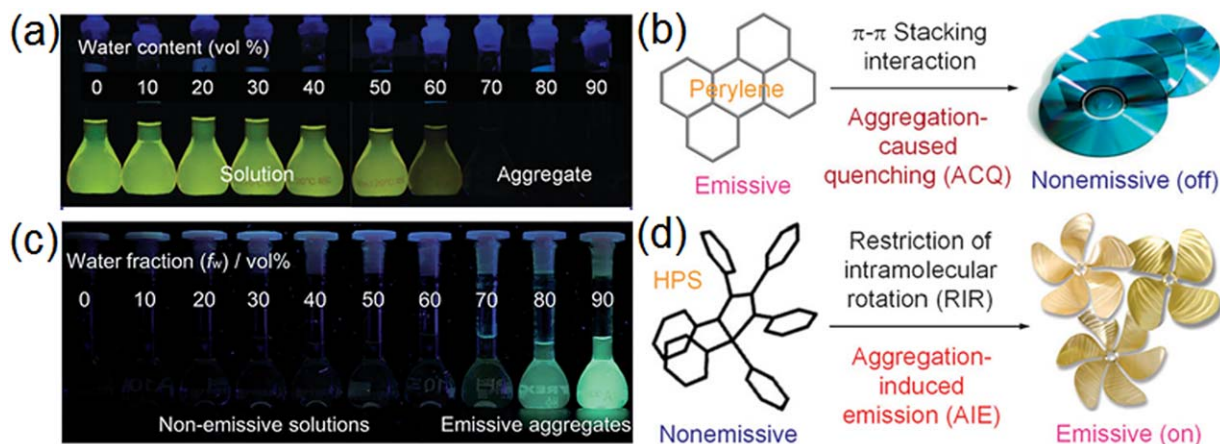


**FIGURE 1** Fluorescence photographs of solutions/suspensions of (a) DDPD (10  $\mu$ M) and (c) HPS (20  $\mu$ M) in THF/water mixtures with different water contents. (b) Planar fluorescent molecules (e.g. perylene) tend to aggregate like discs stack up due to the strong  $\pi$ - $\pi$  interactions between the aromatic rings. (d) Nonplanar HPS molecules have a propeller-shaped structure, which prevents  $\pi$ - $\pi$  stacking and promotes RIR effect in aggregate state. Reproduced from Refs. 3 and 4, with permission from The Royal Society of Chemistry (2009 and 2015).

A2HPS-HCl from the GO substrate, producing the RIR-induced fluorescence emission by trapping it into the dsDNA [Fig. 2(a)]. Unlike dsDNA, the interactions of other biomolecules (e.g. RNA and BSA) with A2HPS-HCl are not strong enough to pull the adsorbed A2HPS-HCl away from the GO substrate. As such, the GO-supported A2HPS-HCl can selectively detect dsDNA [Fig. 2(b)]. The interactions between AIE molecules and biomolecules can be tuned by simply changing the molecular structure of the AIE probes, leading to selective detection of specific biomolecules. Hence, this methodology developed by Tang and coworkers can be regarded as a general approach to the design and development of AIE-based biosensors with a high sensitivity and selectivity.<sup>24</sup>

The above-mentioned RIR mechanism developed by Tang et al. for biosensing with small AIE molecules has also been

applied to the development of water soluble AIE polymers as biosensors.<sup>13</sup> Among them, polyelectrolytes with AIE characteristics are mostly explored.<sup>16,17</sup> By taking advantage of complexation-induced aggregation of a conjugated poly(pyridinium salt), Sun et al. developed a fluorescence turn-on biosensor for detection and quantification of DNA.<sup>16</sup>

Subsequently, Wang et al. synthesized a novel AIE polycation (P(PMVP-co-MVP)) by quaternization of poly(4-vinylpyridine) (P4VP) with bromomethyl-perylene and methyl iodide [inset of Fig. 3(b)].<sup>17</sup> In this polycation, the pyridine moiety acts as  $\pi$ -conjugated stator and the perylene as  $\pi$ -conjugated rotor. The cationic P(PMVP-co-MVP) and anionic ssDNA could form a complex probe for the detection of DNA hybridization [Fig. 3(a)]. Upon adding noncomplementary ssDNA, the fluorescence of the complex probe increased due to the AIE effect.

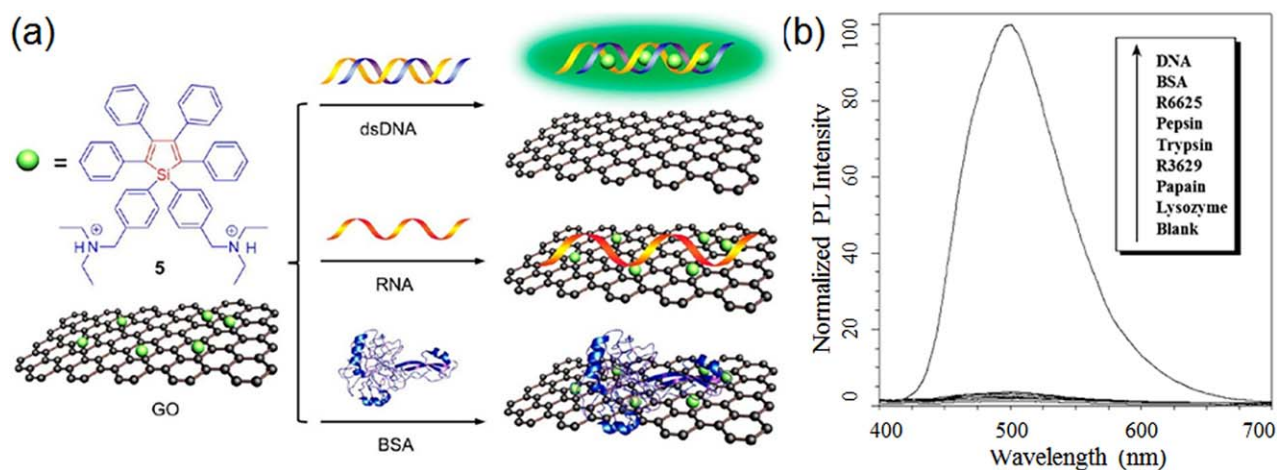


**FIGURE 2** (a) Schematic illustration of selective detection of dsDNA by A2HPS-HCl with the aid of GO. Reproduced with permission from Ref. 2, with permission from American Chemical Society (2013). (b) Fluorescence spectra of GO-A2HPS-HCl upon addition of various biomolecules. Reproduced from Ref. 23, with permission from Wiley-VCH Verlag GmbH & Co. KGaA, Weinheim (2012).

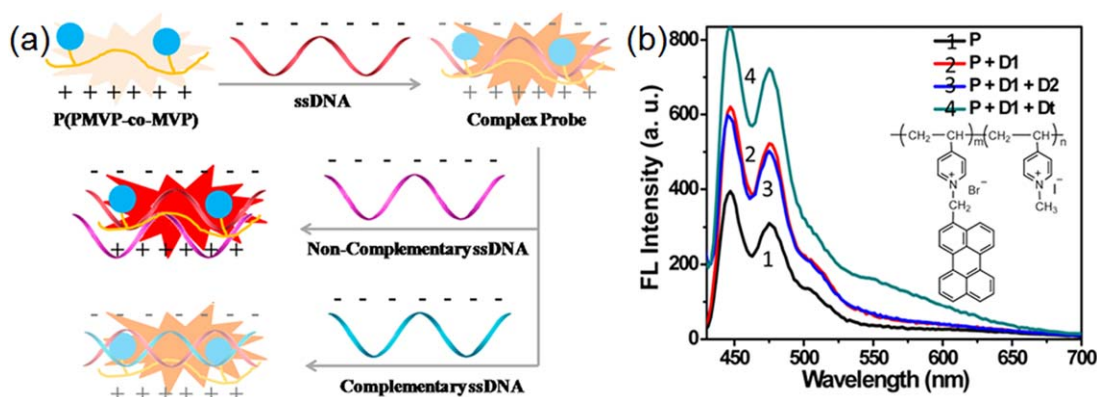


**FIGURE 3** (a) Conceptual illustration of the complex probe formation and label-free DNA detection based on AIE and DNA hybridization. (b) Fluorescence spectra of the polymer and its complexes with different DNA molecules. P, D1, D2, and Dt stand for P(PMVP-co-MVP), ssDNA, complementary ssDNA, and noncomplementary ssDNA, respectively. Reproduced from Ref. 17, with permission from American Chemical Society (2014).

When adding complementary ssDNA, the fluorescence intensity changed little [Fig. 3(b)]. This is because although the AIE effect caused by the addition of anionic complementary ssDNA will enhance the fluorescence, the intercalation of perylene moieties into the duplex could quench some fluorescence.<sup>17</sup> As a result, the neat change of fluorescence was not obvious. This AIE-based strategy for detecting DNA hybridization points out a valuable direction for the application of AIE polymers in bioassays.

#### AIE-Based Fluorescent Cell Imaging

Fluorescent probes that can selectively illuminate specific organelle are highly desirable for studying cellular processes.<sup>25–35</sup> For long time observation of dynamic changes within living cells, the fluorescent probe used must be photostable under continuous irradiation of the exciting light.<sup>2,29</sup> To avoid the ACQ effect, however, conventional fluorescent dyes for organelle staining need to be used in dilute solutions, in which the dye molecules are susceptible to photobleaching by the strong excitation light (*vide supra*).<sup>2</sup> In contrast, AIE fluorogens form nanoaggregates at higher concentrations to become stronger fluorescent emitter, which has also a better photostability than individual fluorescent molecules in dilute solution. This is because the nanoaggregate structure could protect the inner AIE molecules from being further photobleached even when the molecules on the nanoparticle surface are somewhat damaged.<sup>2</sup> Compared with molecular probes, the nanoaggregates can be more easily internalized into cells through endocytosis<sup>11</sup> and should be better fluorescent probes for organelle staining. To achieve selectivity to a specific organelle, however, AIE fluorogens need to be functionalized with organelle targeting moieties. For this purpose, triphenylphosphonium (TPP) can be used to carry molecular probes into mitochondria *via* organelle-specific hydrophobic and electrostatic interactions.<sup>25</sup> By functionalizing TPE with TPP, the resultant TPE-TPP can specifically stain mitochondria within live cells.<sup>25</sup> An isothiocyanate (NCS) moiety can be introduced in the AIE fluorogen to covalently conjugate it with mitochondrial proteins to further

enhance the specific interaction between the AIE probe and mitochondria.<sup>28</sup> Consequently, the as-prepared TPE-Py-NCS can selectively light up the mitochondrial region of HeLa cells through bright yellow fluorescence emission [Fig. 4(a)]. The image from TPE-Py-NCS staining shown in Figure 4(a) is a close replication of that from a commercially available mitochondrial imaging agent, MitoTracker Red CMCros (MTR) [Fig. 4(b)], indicating that TPE-Py-NCS can indeed selectively target mitochondria. The covalent conjugation of the fluorescent probe to mitochondrial proteins, as demonstrated by Zhang et al.,<sup>28</sup> has significantly enhanced the resistance to microenvironmental changes for real-time monitoring of mitophagy behavior.

To demonstrate the general applicability of AIE probes for specific organelle imaging, TPE was also decorated with dimethylamine and malonitrile (TPE-AC) to selectively stain lipid droplets (LDs).<sup>36</sup> As reference, a commercially available imaging agent for LDs (i.e. BODIPY 493/503) was used to co-stain the oleic acid-treated HeLa cells. The similarity between the fluorescence images shown in Figure 4(d,e) suggests that both TPE-AC and BODIPY 493/503 stained the LDs within cells. A clear image of LDs with a considerably high signal-to-noise ratio could be obtained for the TPE-AC fluorescent probe at a staining time as short as 15 min. When the concentration of TPE-AC was increased up to 100  $\mu\text{M}$ , the staining process could be shortened to 2 min. These results indicate that TPE-AC could pass through the cell membrane easily and stain the LDs inside the cell rapidly. As shown in Figure 4(f), there was no significant signal loss for TPE-AC after 80 scans, but more than half of the fluorescence intensity from BODIPY 493/503 was lost after 40 scans. Clearly, therefore, TPE-AC has a much higher photostability than that of BODIPY 493/503.

Recently, Leung et al. attached the lysosome-targeting morpholine group (LysoY) to a FAS-Br chromophore.<sup>37</sup> The resultant AIE-LysoY molecule showed little cytotoxicity and could selectively accumulate in the lysosome of HeLa cells to light it up [Fig. 4(g)]. Compared with the conventional lysosome-

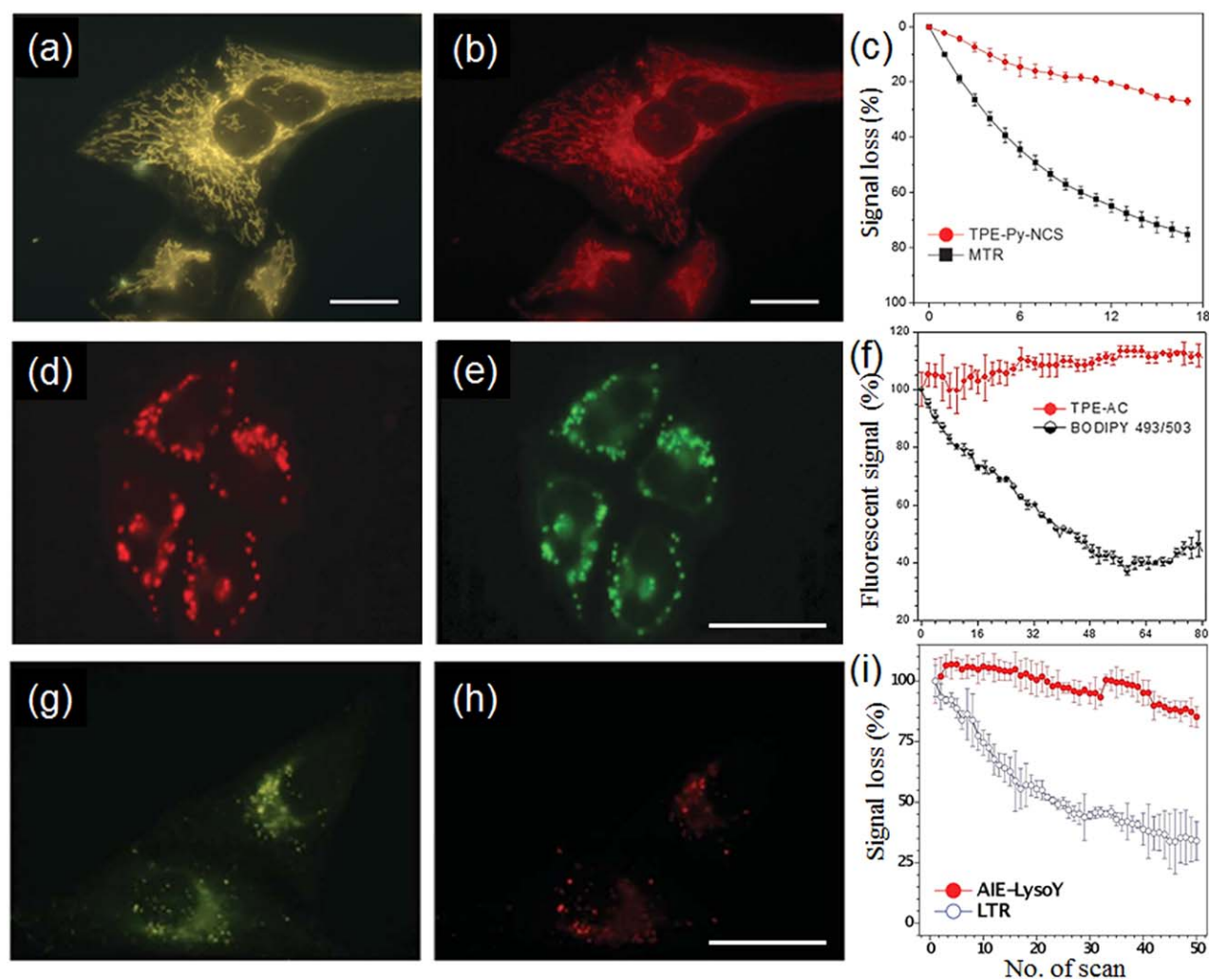


**FIGURE 4** Fluorescent images of HeLa cells stained with (a) TPE-Py-NCS and (b) MitoTracker Red CMXRos (MTR), (c) Loss of fluorescence with the number of scans, Reproduced from Ref. 28, with permission from The Royal Society of Chemistry (2015); fluorescent images of HeLa cells stained with (d) TPE-AC and (e) BODIPY 493/503, (f) loss of fluorescence with the number of scans of laser irradiation, Reproduced from Ref. 36, with permission from The Royal Society of Chemistry (2016); fluorescent images of HeLa cells stained with (g) AIE-LysoY and (h) LysoTracker Red (LTR), (i) loss of fluorescence with increasing number of scans. Scale bars in (a) and (b) are 20  $\mu\text{m}$ , others are 30  $\mu\text{m}$ . Reproduced from Ref. 37, with permission from of Wiley-VCH Verlag GmbH & Co. KGaA, Weinheim (2015).

targeting probe (i.e. LysoTracker Red DND-99, LTR), AIE-LysoY had a higher affinity to lysosome and exhibited a higher contrast [Fig. 4(g,h)] and a better photostability [Fig. 4(i)]. After continuous scanning for 50 times, the fluorescence signal from AIE-LysoY decreased only a bit [Fig. 4(i)], confirming its excellent photostability. In contrast, about 50% fluorescence intensity of LTR was lost after only 25 scans [Fig. 4(i)]. As mentioned above, the excellent photostability of AIE-LysoY stemmed from its nanoparticle structure, which can protect the chromophore inside the particles from being readily photooxidized.<sup>37</sup> Thus, the photostable AIE-LysoY holds potentials for real-time tracking biological processes of lysosome.

Compared with nanoaggregates formed by small AIE molecules, AIE polymer nanoparticles exhibit a series of superior

characteristics for cell imaging applications, including good water dispersibility, excellent biocompatibility, high cell permeability, and multifunctionality.<sup>18–21,38</sup> By introducing a pH-sensitive green AIE fluorogen and a nonresponsive blue AIE fluorogen as reference into a hyperbranched polymer [Fig. 5(a)], Bao et al. realized cell imaging and intracellular pH mapping simultaneously.<sup>18</sup> These polymer nanoparticles could selectively accumulate in the acidic organelles of living cells by endocytosis process with no obvious cytotoxicity.<sup>18</sup> The fluorescence from the green AIE fluorogens increased dramatically with reduction of pH values, whereas that from the blue AIE fluorogens slowly altered.<sup>18</sup> As seen in Figure 5(b), therefore, the intensity ratio ( $I_{\text{green}}/I_{\text{blue}}$ ) displayed a unique pH dependence for pH sensing. For instance, the pH values of spots 1 and 2 in the fluorescence image of HeLa cells were determined to be  $6.0 \pm 0.2$  and  $5.2 \pm 0.2$ ,

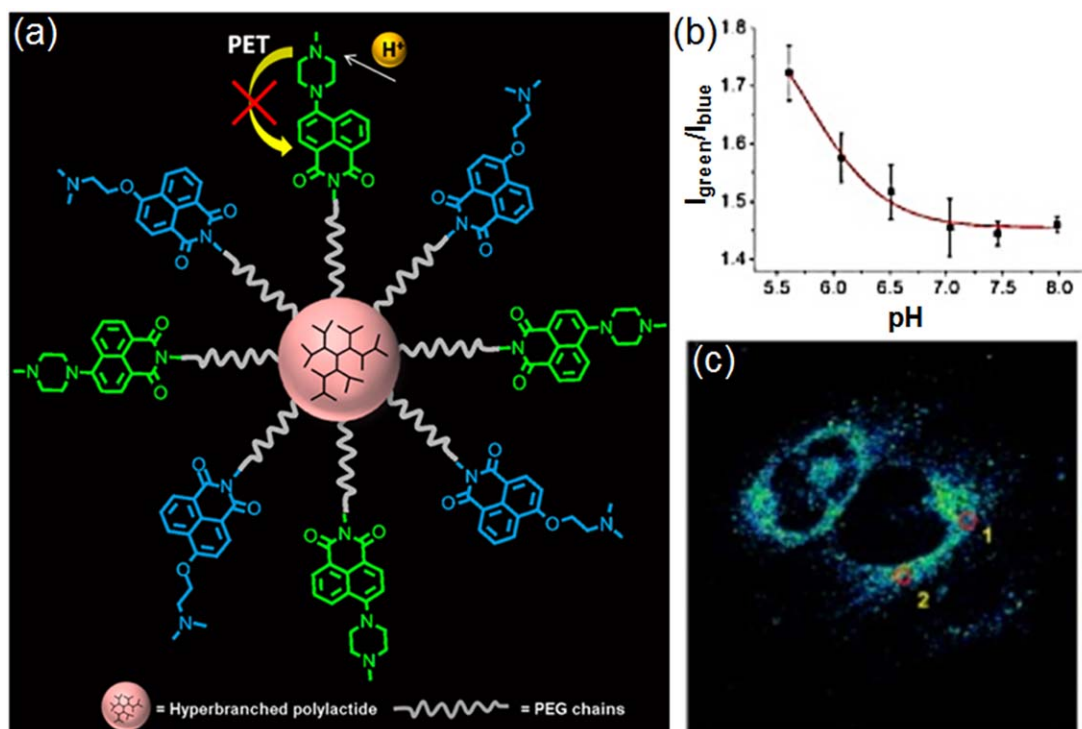


**FIGURE 5** (a) Hyperbranched poly(lactide) nanoparticles functionalized with a green emissive AIE fluorophore as pH sensitive probe and a blue emissive AIE fluorophore as reference; (b) The calibration curve about the relation between  $I_{\text{green}}/I_{\text{blue}}$  and pH obtained using nigericin; (c) The pH map for untreated HeLa cells based on the curve in (b). Reproduced from Ref. 18, with permission from Copyright of American Chemical Society (2015).

respectively [Fig. 5(c)]. These were the expected values for acidic organelles, endosomes and lysosomes. Therefore, these hyperbranched AIE polymer nanoparticles could be used as an efficient sensing platform for simultaneous organelle imaging and intracellular pH mapping in living cells.

## CONCLUSIONS

Aggregation caused quenching (ACQ) has been studied for many years whereas the aggregation-induced emission (AIE) is a recent development. Since Tang discovered AIE in 2001, tremendous progress has been achieved. AIE fluorogens are nearly nonemissive in molecular states with their intermolecular rotations being not restricted, but their fluorescences turn on upon aggregation or binding with certain biomolecules, which restrict the intramolecular rotation of the fluorogens. Through judicious functionalization of AIE fluorogens with hydrophilic and/or targeting moieties or incorporating them into polymeric structures, they can be used for turn-on fluorescent biosensing and organelle-specific imaging with a high sensitivity and selectivity. Compared with ACQ molecular probes, AIE nanoaggregates have a higher photostability and can be more easily internalized into cells through endocytosis for real time monitoring the dynamic life processes in living cells. However, the ultraviolet light, which is harmful to cells and may change the cell behavior or even kill cells, is usually needed to excite the AIE fluorogens. Thus, recent development of AIE bioprobes has focused on AIE fluorogens

with two-photon or multiphoton absorption capabilities so that two or multiple visible or near infrared photons of low energy can be used as the excitation light,<sup>39,40</sup> which could also have a higher penetration depth than that of ultraviolet light for *in vivo* cell or tissue sensing and imaging. Continued research in this exciting field pioneered by Ben Zhong Tang would be of great value.

## ACKNOWLEDGMENTS

The authors are grateful for the financial support from NSF, NSF-NSFC, AFOSR-DoD-MURI, DAGSI.

## REFERENCES AND NOTES

- 1 K. Th. Förster, Z. Kasper, *Phys. Chem. (Munich)* **1954**, *1*, 275–277.
- 2 D. Ding, K. Li, B. Liu, B. Z. Tang, *Acc. Chem. Res.* **2013**, *46*, 2441–2453.
- 3 Y. Hong, J. W. Y. Lam, B. Z. Tang, *Chem. Soc. Rev.* **2011**, *40*, 5361–5388.
- 4 Z. J. Zhao, B. R. He, B. Tang, *Chem. Sci.* **2015**, *6*, 5347–5365.
- 5 Y. Hong, J. W. Lam, B. Z. Tang, *Chem. Commun.* **2009**, 4332–4353.
- 6 J. Luo, Z. Xie, J. W. Y. Lam, L. Cheng, H. Chen, C. Qiu, H. S. Kwok, X. Zhan, Y. Liu, D. Zhu, B. Z. Tang, *Chem. Commun.* **2001**, 1740–1741.

- 7** J. Mei, N. L. Leung, R. T. Kwok, J. W. Lam, B. Z. Tang, *Chem. Rev.* **2015**, *115*, 11718–11940.
- 8** F. Bu, R. Duan, Y. Xie, Y. Yi, Q. Peng, R. Hu, A. Qin, Z. Zhao, B. Z. Tang, *Angew. Chem. Int. Ed.* **2015**, *54*, 14492–14497.
- 9** A. T. Han, H. M. Wang, R. T. K. Kwok, S. L. Ji, J. Li, D. L. Kong, B. Z. Tang, B. Liu, Z. M. Yang, D. Ding, *Anal. Chem.* **2016**, *88*, 3872–3878.
- 10** Z. G. Song, R. T. K. Kwok, D. Ding, H. Nie, J. W. Y. Lam, B. Liu, B. Z. Tang, *Chem. Commun.* **2016**, *52*, 10076–10079.
- 11** D. Ding, R. T. K. Kwok, Y. Yuan, G. Feng, B. Z. Tang, B. Liu, *Mater. Horiz.* **2015**, *2*, 100–105.
- 12** M. E. Jun, B. Roy, K. H. Ahn, *Chem. Commun.* **2011**, *47*, 7583–7601.
- 13** R. Hu, Y. Kang, B. Z. Tang, *Polym. J.* **2016**, *48*, 359–370.
- 14** R. Hu, N. L. C. Leung, B. Z. Tang, *Chem. Soc. Rev.* **2014**, *43*, 4494–4562.
- 15** R. Hu, J. W. Y. Lam, M. Li, H. Deng, J. Li, B. Z. Tang, *J. Polym. Sci. Part A: Polym. Chem.* **2013**, *51*, 4752–4764.
- 16** J. Sun, Y. Lu, L. Wang, D. Cheng, Y. Sun, X. Zeng, *Polym. Chem.* **2013**, *4*, 4045–4051. –
- 17** G. Wang, R. Zhang, C. Xu, R. Zhou, J. Dong, H. Bai, X. Zhan, *ACS Appl. Mater. Interfaces* **2014**, *6*, 11136–11141.
- 18** Y. Bao, H. D. Keersmaecker, S. Corneillie, F. Yu, H. Mizuno, G. Zhang, J. Hofkens, B. Mendrek, A. Kowalczyk, M. Smet, *Chem. Mater.* **2015**, *27*, 3450–3455.
- 19** X. Zhang, X. Zhang, B. Yang, J. Hui, M. Liu, Z. Chi, S. Liu, J. Xu, Y. Wei, *Polym. Chem.* **2014**, *5*, 683–688.
- 20** K. Wang, X. Zhang, X. Zhang, C. Ma, Z. Li, Z. Huang, Q. Zhang, Y. Wei, *Polym. Chem.* **2015**, *6*, 4455–4461.
- 21** K. Wang, X. Zhang, X. Zhang, B. Yang, Z. Li, Q. Zhang, Z. Huang, Y. Wei, *Polym. Chem.* **2015**, *6*, 1360–1366.
- 22** Y. Dong, J. W. Y. Lam, A. Qin, Z. Li, J. Liu, J. Sun, Y. Dong, B. Z. Tang, *Chem. Phys. Lett.* **2007**, *446*, 124–127.
- 23** X. J. Xu, J. J. Li, Q. Q. Li, J. Huang, Y. Q. Dong, Y. N. Hong, J. W. Yan, J. G. Qin, Z. Li, B. Z. Tang, *Chem. Eur. J.* **2012**, *18*, 7278–7286.
- 24** Q. Q. Li, Z. Li, *Sci. China Chem.* **2015**, *58*, 1800–1809.
- 25** C. W. Leung, Y. Hong, S. Chen, E. Zhao, J. W. Lam, B. Z. Tang, *J. Am. Chem. Soc.* **2013**, *135*, 62–65.
- 26** E. Wang, E. Zhao, Y. Hong, J. W. Y. Lam, B. Z. Tang, *J. Mater. Chem. B* **2014**, *2*, 2013–2019.
- 27** X. Gu, E. Zhao, J. W. Lam, Q. Peng, Y. Xie, Y. Zhang, K. S. Wong, H. H. Sung, I. D. Williams, B. Z. Tang, *Adv. Mater.* **2015**, *27*, 7093–7100.
- 28** W. Zhang, R. T. K. Kwok, Y. Chen, S. Chen, E. Zhao, C. Y. Y. Yu, J. W. Y. Lam, Q. Zheng, B. Z. Tang, *Chem. Comm.* **2015**, *51*, 9022–9025.
- 29** S. J. Chen, H. Wang, Y. N. Hong, B. Z. Tang, *Mater. Horiz.* **2016**, *3*, 283–293.
- 30** X. G. Gu, E. G. Zhao, T. Zhao, M. M. Kang, C. Gui, J. W. Y. Lam, S. W. Du, M. M. T. Loy, B. Z. Tang, *Adv. Mater.* **2016**, *28*, 5064–5071.
- 31** C. Y. Y. Yu, W. J. Zhang, R. T. K. Kwok, C. W. T. Leung, J. W. Y. Lam, B. Z. Tang, *J. Mater. Chem. B* **2016**, *4*, 2614–2619.
- 32** Z. Wang, C. Gui, E. Zhao, J. Wang, X. Li, A. Qin, Z. Zhao, Z. Yu, B. Z. Tang, *ACS Appl. Mater. Interfaces* **2016**, *8*, 10193–10200.
- 33** Z. G. Song, W. J. Zhang, M. J. Jiang, H. H. Y. Sung, R. T. K. Kwok, H. Nie, I. D. Williams, B. Liu, B. Z. Tang, *Adv. Funct. Mater.* **2016**, *26*, 824–832.
- 34** B. Situ, S. Chen, E. Zhao, C. W. T. Leung, Y. Chen, Y. Hong, J. W. Y. Lam, Z. Wen, W. Liu, W. Zhang, L. Zheng, B. Z. Tang, *Adv. Funct. Mater.* **2016**, *26*, 7132–7138.
- 35** C. Y. W. Lo, S. Chen, S. J. Creed, M. Kang, N. Zhao, B. Z. Tang, K. D. Elgass, *Sci. Rep.* **2016**, *6*, 30855.
- 36** M. M. Kang, X. G. Gu, R. T. K. Kwok, C. W. T. Leung, J. W. Y. Lam, F. Li, B. Z. Tang, *Chem. Commun.* **2016**, *52*, 5957–5960.
- 37** C. W. T. Leung, Z. M. Wang, E. G. Zhao, Y. N. Hong, S. J. Chen, R. T. K. Kwok, A. C. S. Leung, R. S. Wen, B. S. Li, J. W. Y. Lam, B. Z. Tang, *Adv. Healthcare Mater.* **2016**, *5*, 427–431.
- 38** X. Zhang, X. Zhang, B. Yang, Y. Yang, Y. Wei, *Polym. Chem.* **2014**, *5*, 5885–5889.
- 39** Z. F. Chang, L. M. Jing, B. Chen, M. S. Zhang, X. L. Cai, J. J. Liu, Y. C. Ye, X. D. Lou, Z. J. Zhao, B. Liu, J. L. Wang, B. Z. Tang, *Chem. Sci.* **2016**, *7*, 4527–4536.
- 40** B. Chen, G. X. Feng, B. R. He, C. Goh, S. D. Xu, G. Ramos-Ortiz, L. Aparicio-Ixta, J. Zhou, L. G. Ng, Z. J. Zhao, B. Liu, B. Z. Tang, *Small* **2016**, *12*, 782–792.